

March 2007  
hep-th/0703104

## On the Singularities of the Magnon S-matrix

Nick Dorey<sup>1</sup>, Diego M. Hofman<sup>2</sup> and Juan Maldacena<sup>3</sup>

<sup>1</sup>DAMTP, University of Cambridge, Cambridge CB3 0WA, UK.

<sup>2</sup> Joseph Henry Laboratories, Princeton University, Princeton, NJ 08544, USA.

<sup>3</sup> Institute for Advanced Study, Princeton NJ 08540, USA.

### Abstract

We investigate the analytic structure of the magnon S-matrix in the spin-chain description of planar  $\mathcal{N} = 4$  SUSY Yang-Mills/ $AdS_5 \times S^5$  strings. Semiclassical analysis suggests that the exact S-matrix must have a large family of poles near the real axis in momentum space. In this article we show that these are double poles corresponding to the exchange of pairs of BPS magnons. Their locations in the complex plane are uniquely fixed by the known dispersion relation for the BPS particles. The locations precisely agree with the recent conjecture for the  $S$  matrix by Beisert, Hernandez, Lopez, Eden and Staudacher (hep-th/0609044 and hep-th/0610251). These poles do not signal the presence of new bound states. In fact, a certain non-BPS localized classical solution, which was thought to give rise to new bound states, can actually decay into a pair of BPS magnons.

# 1 Introduction

In 't Hooft's large  $N$  limit, a gauge theory is reduced to the sum of planar diagrams. These diagrams give rise to a two dimensional effective theory which is supposed to be the worldsheet of a string. A great deal of effort has been devoted recently to studying planar  $\mathcal{N} = 4$  super Yang Mills, culminating in a conjecture for the exact  $\lambda = g^2 N$  dependence of some quantities [1, 2] (see also [3]). This has been done using the assumption of exact integrability plus other reasonable assumptions. The quantity that has been conjectured is the exact  $S$  matrix describing the scattering of worldsheet excitations. Let us briefly describe how this quantity is defined in the gauge theory [4]. In  $\mathcal{N} = 4$  super Yang mills we have an  $SO(6)$  R-symmetry. We pick an  $SO(2)$  subgroup generated by  $J = J_{56}$ . We denote by  $Z$  the scalar field that carries charge one under  $J$ . We then consider single trace local operators with very large charge,  $J \rightarrow \infty$ , and conformal dimension,  $\Delta$ , close to  $J$ , so that  $\Delta - J$  is finite in the limit. In this limit the local operator contains a large number of fields  $Z$  and a finite number of other fundamental fields. These  $Z$  fields form a sort of one dimensional lattice on which the other fields propagate. It turns out that we can describe all the other fields in terms of a set of 8 bosonic and 8 fermionic fundamental fields [5]. The 8 bosonic ones are four of the scalar fields that are not charged under  $J$  and the four derivatives of  $Z$ ,  $\partial_\mu Z$ . We can view the different fields at each site as a generalized spin. Therefore, we are dealing with a generalized spin chain. For this reason the fundamental excitations are often called "magnons". The symmetry algebra acting on an infinite chain is enhanced in such a way that the fundamental excitations (or magnons) are BPS for all values of their momenta [6].

This symmetry also completely constrains the matrix structure of the  $2 \rightarrow 2$  scattering amplitude [6]. Only the overall phase is undetermined. The phase is constrained by a crossing symmetry equation [7, 8]. Recently, an expression for this phase, sometimes called "dressing factor" [9], was proposed in [1, 2]. The proposed phase is a non-trivial function of the 't Hooft coupling  $\lambda$  and is supposed to be valid for all values of this parameter. The function also depends on the two momenta of the particles  $p_1, p_2$  and can be analytically continued to complex values of these variables. As we do so, we encounter poles and branch points. In this article we explore the physical meaning of some poles that appear when we perform this analytic continuation. For  $S$  matrices in any dimension, simple poles are

typically associated to on shell intermediate states. In fact, such simple poles appear in some of the matrix elements of the full matrix  $S$  and are independent of the dressing factor. They were interpreted as BPS bound states for single magnon excitations in [10]. It turns out that one can have BPS bound states of  $n$  fundamental magnons for any positive integer  $n$ . Further poles were necessary in order to account for branch cuts in the scattering of magnons in the classical limit considered in [14]. In the proposal of [1, 2] these turn out to be double poles. Such double poles do not arise from bound states and look a bit puzzling at first sight. However, similar double poles appear in the  $S$  matrix for sine Gordon theory and their physical origin was elucidated by Coleman and Thun [15] (see [16] for a recent review on two dimensional S-matrices). In short, they arise from physical processes where the elementary particles exchange pairs of particles rather than a single particle. In higher dimensions such processes give rise to branch cuts, but they give double poles in two dimensions. The precise position of these double poles depends on the dispersion relation for the exchanged particles. If we assume that the exchanged particles are the BPS magnon bound states discussed above we find that the double poles appear precisely where the conjecture of [1, 2] predicts them. Thus, this computation can be viewed as a check of their proposal, since it has singularities where (with hindsight) one would have expected them.

More generally, the existence of the singularities dictated by the spectrum (and no others in the physical region) provides extra constraints on the S-matrix beyond those of unitarity, crossing and factorizability. As in relativistic models [17], these constraints help to remove ambiguities associated with the homogeneous solutions of the crossing equations. Optimistically, one can hope that this type of reasoning might provide a physical basis for selecting the conjectured S-matrix of [2] from the many possible solutions to the crossing equation.

In [14] some non-BPS localized classical solutions were found and it was suggested that they could correspond to non-BPS bound states. If true this would mean that the S-matrix should have single poles rather than double poles. These solutions move in an  $R \times S^2$  subspace of the full  $AdS_5 \times S^5$  theory and within this subspace they are stable. Here we show that these solutions can decay once they are embedded in  $AdS_5 \times S^5$ . In fact these solutions can be viewed as a non-BPS superposition of two coincident BPS magnons with large  $n$  and the same momentum. The decay of the solutions corresponds to these two BPS magnons moving away from each other. Our results suggest that the only single-particle asymptotic

states of the theory are the tower of BPS boundstates described in [10, 11, 12, 13].

This article is organized as follows. In Section two we review Coleman and Thun's explanation for the double poles. In Section three we use the magnon dispersion relation to give the location of the double poles. In Section four we discuss the localized classical solutions found in [14, 18] and their relation to the double poles. We also discuss a slow relative velocity limit, or non-relativistic limit, where the system seems to simplify. In particular we present a toy model, in this limit, which reproduces some of the features of the full theory. In Section five we compute the location of the double poles in the recent conjecture of [1, 2]. The derivation of a useful integral representation of the conjectured phase is given in an Appendix. Finally, we include two other Appendices where we present some diagrams related to the double poles and where we include explicitly the classical solutions of [18].

## 2 S-matrix Singularities

Since the S-matrix is a physical observable, its singularities should have a physical explanation. In fact, S-matrix singularities arise when we produce on shell particles that propagate over long distances or long times. Thus the singularities are interpreted as an IR phenomenon associated to the propagation of particles.

Let us consider a  $2 \rightarrow 2$  scattering process. The simplest and most familiar example is a single pole. These poles arise when an intermediate on shell particle is produced in the collision. See Figure 1(a).

If we have more than one particle becoming on shell we can have other types of singularities. The simplest example is a two particle threshold, where we can start producing a pair of intermediate on-shell particles, see Figure 1(b). For our purposes we will need to consider more complicated cases. This problem was studied by Landau [19] who found the general rules for locating the singularities. The singularities correspond to spacetime graphs where the vertices are points in spacetime, representing local interaction regions. Lines are on shell particles with particular momenta  $p^\mu$  and the spacetime momenta are conserved at the vertices. In addition, the four momentum of the line connecting two vertices obeys  $x_2^\mu - x_1^\mu = \alpha p^\mu$ , with  $\alpha > 0$  (there is one  $\alpha$  for each internal line). Thus, the singularity is

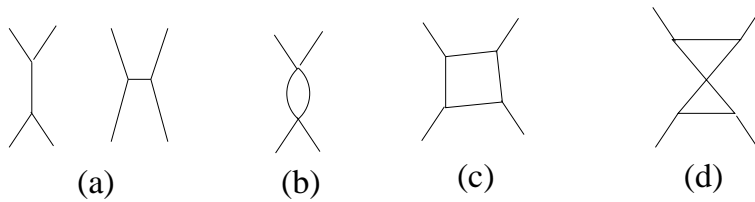


Figure 1: Diagrams associated to singularities of the S-matrix.

associated to the physical propagation of these on shell particles. Notice that this condition implies that if the energy  $p^0$  is positive, then  $x_2^0 > x_1^0$ , so that the particle is going forwards in time. More details can be found in [20, 21]. The type of singularity that we obtain depends on the dimension, since we generally have integrals over loop momenta. We typically encounter branch points<sup>1</sup>. For the box diagram in Figure 1(c) we have a  $D$  dimensional loop integral and one mass shell delta function for each line. We expect a divergence in  $D < 4$  dimensions and branch points for  $D \geq 4$ . In two dimensions,  $D = 2$ , we naively get the square of a delta function at zero. A more careful analysis reveals that we get a double pole [15, 21]. Other graphs, such as the two loop diagram in Figure (1)(d), also give rise to double poles. In two dimensions we get double poles in diagrams with  $L$  loops and  $N$  internal lines when  $N - 2L = 2$ .

So far, we were assuming that the singularities arise for real values of the external momenta. On the other hand, it is often the case that the singularities only arise when we perform an analytic continuation in the external momenta. The spacetime points discussed above now live in a complexified spacetime. If we are interested in the “first” singularity that appears as we move away from the physical sheet, it is sufficient to consider momenta which are in “anti-Euclidean” space where  $p^0$  is real and  $p^i$  are purely imaginary [21]. As we go through branch cuts we can encounter additional singularities which relax some of the rules discussed above. In particular, we can relax the condition that the  $\alpha$ ’s for each line are positive. Here we will be interested in the first singularity that arises and not on the ones that are on other sheets. In two dimensions, the energy and momentum conservation conditions and the on shell conditions for all internal lines determine the energies and momenta up to some discrete options. At any of these values we will have a singularity in some sheet. If we are interested in the “first” or physical sheet singularities then we need to impose a the further condition

---

<sup>1</sup>The discontinuity across the branch cut emanating from it can be evaluated using the Cutkosky rules[20].

that the  $\alpha_i$  discussed above are positive, or equivalently, that the graph in “anti-Euclidean” space closes. This selects a subset of all the discrete solutions to the energy and momentum conservation conditions.

In our case, we do not have a relativistic theory, so we do not know a priori how much we can analytically continue the amplitudes and expect to find a physical explanation for all singularities. However, since the origin of the singularities is an IR phenomenon we expect that the discussion should also hold for spin chains. Understanding precisely the whole physical region is beyond the scope of this paper. Here we will perform the analytic continuation only within a very small neighborhood of the real values looking for the “first” singularities. As we explained above, after we impose the momentum and energy conservation conditions we will be left with discrete possible solutions. We should select among them to find the singularities that are on the physical sheet. We are not going to give a general rule, as was given for relativistic theories. Instead we are going to analyze mainly two cases in this paper. In the first case we will be scattering particles in the near plane wave region where particles are approximately relativistic and we can apply the relativistic rules in order to check whether the singularity is on the first sheet or not. The second case is when the particles we scatter are in the giant magnon region. In this case we can use a slow motion, non relativistic approximation plus some physical arguments regarding the interpretation of the solutions in order to select among different solutions.

### 3 Poles from physical processes

As discussed above, the singularities of the S-matrix correspond to different on-shell intermediate states. In particular, the location and nature of the singularities are essentially determined once the spectrum of the theory is known. To understand the poles of the magnon S-matrix we therefore begin by reviewing the spectrum of the  $\mathcal{N} = 4$  spin chain.

The fundamental excitations of the spin chain are the magnons themselves, which lie in a sixteen-dimensional BPS representation of the unbroken  $SU(2|2) \times SU(2|2)$  supersymmetry. The closure of the SUSY algebra on this multiplet uniquely determines [6] the magnon

dispersion relation to be [22] (see also [23]),

$$E = \Delta - J = \sqrt{1 + 16g^2 \sin^2 \left(\frac{p}{2}\right)} \quad (1)$$

where  $g = \sqrt{g_{YM}^2 N}/4\pi$ . In addition, any number of elementary magnons can form a stable boundstate. The  $n$ -magnon boundstate also lies in a BPS representation of supersymmetry (of dimension  $16n^2$ ). The theory therefore contains an infinite tower of BPS states labelled by a positive integer  $n$ . The exact dispersion relation for these states is again fixed by supersymmetry to be [10, 13],

$$E = \Delta - J = \sqrt{n^2 + 16g^2 \sin^2 \left(\frac{p}{2}\right)} \quad (2)$$

The existence of these states can be confirmed both in the gauge theory spin-chain and in the string world-sheet theory for appropriate values of the coupling [10]. It remains possible that there are additional boundstates in the theory which are not BPS. However we will see that we have no reason to introduce them, at least if one believes in the recently conjectured  $S$  matrix in [1, 2]. In fact, the poles in this proposed result can be accounted for by thinking about physical processes involving the set of BPS states described above.

## Kinematics

The dispersion relation (2) for an arbitrary BPS state is conveniently written in terms of complex spectral parameters,

$$X^\pm = e^{\pm ip/2} \frac{\left(n + \sqrt{n^2 + 16g^2 \sin^2 \left(\frac{p}{2}\right)}\right)}{4g \sin \left(\frac{p}{2}\right)} \quad (3)$$

which obey the constraint,

$$\left(X^+ + \frac{1}{X^+}\right) - \left(X^- + \frac{1}{X^-}\right) = \frac{in}{g} \quad (4)$$

In terms of these parameters, the particle energy and momentum are given by,

$$E(X^\pm) = \frac{g}{i} \left[ \left(X^+ - \frac{1}{X^+}\right) - \left(X^- - \frac{1}{X^-}\right) \right], \quad p(X^\pm) = \frac{1}{i} \log \left(\frac{X^+}{X^-}\right) \quad (5)$$

These quantities are real provided  $X^+ = (X^-)^*$ . More generally we will consider an analytic continuation of the kinematic variables where the reality condition is relaxed (but the constraint (4) is maintained).

For magnons belonging to an  $SU(2)$  subsector, the integer  $n$  appearing in the constraint (4) corresponds to a conserved  $U(1)$  R-charge. It is convenient to view (4) as giving the charge as a function of the spectral parameters  $n(X^\pm)$ . The velocity of the particle in appropriately-normalised<sup>2</sup> worldsheet coordinates  $(x, t)$  is given as,

$$v = \frac{dx}{dt} = \frac{1}{2g} \frac{dE}{dp} = \frac{X^+ + X^-}{1 + X^+ X^-} = \frac{2g \sin(p)}{\sqrt{n^2 + 16g^2 \sin^2\left(\frac{p}{2}\right)}} \quad (6)$$

and we also define the rapidity parameter,

$$\begin{aligned} u(X^\pm) &= \frac{1}{2} \left[ \left( X^+ + \frac{1}{X^+} \right) + \left( X^- + \frac{1}{X^-} \right) \right] \\ &= \frac{1}{2g} \cot\left(\frac{p}{2}\right) \sqrt{n^2 + 16g^2 \sin^2\left(\frac{p}{2}\right)} \end{aligned} \quad (7)$$

In the strong coupling limit  $g \gg 1$  there are two distinct kinematic regimes which will be of interest. The first is the Giant Magnon regime where the conserved momentum  $p$  is held fixed as  $g \rightarrow \infty$ . We then have

$$E \simeq 4g \sin\left(\frac{p}{2}\right), \quad X^+ \sim \frac{1}{X^-} \sim e^{ip/2}, \quad u \sim 2v \sim 2 \cos\frac{p}{2} \quad (8)$$

These excitations correspond to classical solutions of the worldsheet theory.

The second regime of interest is that of the plane wave limit where we take  $p \rightarrow 0$  as  $g \rightarrow \infty$  with  $k = 2gp$  held fixed. In this case we recover the familiar relativistic relations

$$E \simeq \sqrt{n^2 + k^2}, \quad v = \frac{k}{\sqrt{n^2 + k^2}}, \quad X^+ \sim X^- = \frac{n + E}{k} \sim \frac{n + \sqrt{n^2 + k^2}}{k} \quad (9)$$

These two regimes<sup>3</sup>, (8) and (9), amount to two ways of solving the constraint (4) for large  $g$ , by setting  $X^+ \sim 1/X^-$  or  $X^+ \sim X^-$ .

## S-matrix definitions and conventions

For simplicity, we will consider scattering of two states in the  $SU(2)$  subsector, since the scattering in the other sectors is determined once we know the result in the  $SU(2)$  subsector

---

<sup>2</sup>The normalisation is chosen so that the velocity of light is unity in the plane wave limit discussed below. With this normalization  $p$  generates translations in  $x/(2g)$ .

<sup>3</sup>The two regimes in question are connected by a third, studied in [24, 25] where  $X^\pm \sim 1$  (or  $X^+ \sim X^- \sim -1$ ).



[6]. Of course, we will allow intermediate states to be completely general. We can define the  $S$  matrix (just a complex number in this case) by looking at the wavefunction for two magnons and writing it as

$$\Psi(x_1, x_2) = e^{ip_1x_1 + p_2x_2} + S(p_1, p_2)e^{ip_1x_2 + ip_2x_1}, \quad x_1 \ll x_2 \quad (10)$$

And  $\Psi(x_1, x_2) = \Psi(x_2, x_1)$  for  $x_1 \gg x_2$ , since we have two identical bosons. We see that we can view the first term as the incoming wave and the second as the reflected way if  $v_1 > v_2$ . We will be interested in analytically continuing in the external momenta  $p_i$ . We write then

$$p_1 = p + iq, \quad p_2 = p - iq \quad (11)$$

We will see that the part of the wavefunction depending on the relative coordinate  $x = x_1 - x_2$  has the form  $\Psi \sim e^{-qx} + S(1, 2)e^{qx}$ . Thus we see that the first term diverges as  $x \rightarrow -\infty$  if  $q > 0$ . We set boundary conditions on the non-normalizable piece of the wavefunction, by saying that the coefficient of the exponential is one, and we “measure” the coefficient of the other which is the  $S$  matrix. We then see that a pole of  $S$  (with  $q > 0$ ) can correspond to a bound state.

This  $S$  matrix can be written as

$$S(X_1^\pm, X_2^\pm) = \sigma^{-2}(X_1^\pm, X_2^\pm) \mathcal{S}_{BDS}^{-1}(X_1^\pm, X_2^\pm) \quad (12)$$

where the inverse factors originate from the fact that the conventions for defining the  $S$  matrix in the recent literature are the opposite from ours<sup>4</sup>. The second factor in (12) was originally written in [22] and is

$$\mathcal{S}_{BDS}^{-1}(X_1^\pm, X_2^\pm) = \frac{u(X_1^\pm) - u(X_2^\pm) - i/g}{u(X_1^\pm) - u(X_2^\pm) + i/g} = \frac{(X_1^- - X_2^+)(1 - 1/X_1^- X_2^+)}{(X_1^+ - X_2^-)(1 - 1/X_1^+ X_2^-)} \quad (13)$$

The quantity  $\sigma(X_1^\pm, X_2^\pm)$  is known as the dressing factor and we will discuss the explicit proposal in [1, 2] in Section 5 below. For the moment we will simply use the fact that the proposed dressing factor has no poles or zeros when  $u_1 - u_2 = \pm i$  on the main branch that is closest to physical values.

### 3.1 Simple poles

The singularities of the S-matrix correspond to spacetime diagrams where each particle is on-shell. In general, we will analytically continue to complex values of the momenta

---

<sup>4</sup> Our  $\sigma$  is the same as the  $\sigma$  in [2, 1] and similarly, our  $\mathcal{S}_{BDS}$  is the same S-matrix appearing in [22].

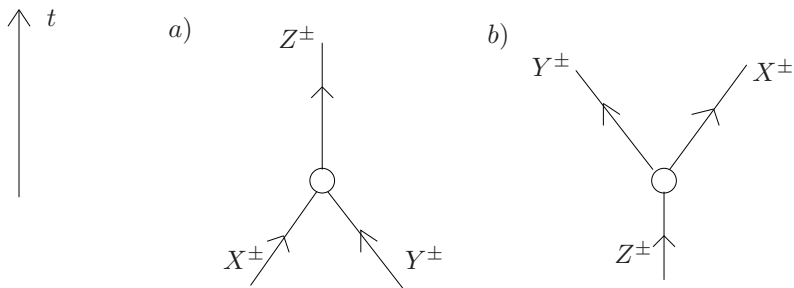


Figure 2: Three-point vertices.

and energies, and thus each particle corresponds to a line in complexified Minkowski space. Particle lines can meet at three-point vertices which conserve charge, energy and momentum. We will now analyze the allowed vertices.

We begin by considering a three point vertex corresponding to the creation of a BPS particle with spectral parameters  $Z^\pm$  from two others with parameters  $X^\pm$  and  $Y^\pm$  as shown in Figure 2a. If all particles belong to the same  $SU(2)$  subsector, then each carries a conserved  $U(1)_R$  charge  $Q = n$ . In this case, the conservation laws for energy, momentum and charge read,

$$\begin{aligned}
 E(X^\pm) + E(Y^\pm) &= E(Z^\pm) \\
 p(X^\pm) + p(Y^\pm) &= p(Z^\pm) \pmod{2\pi} \\
 n(X^\pm) + n(Y^\pm) &= n(Z^\pm)
 \end{aligned}
 \tag{14}$$

The same equations must also hold for the vertex corresponding to the time-reversed process shown in Figure 2b. As the dependence of each conserved quantity on the spectral parameters is of the form  $f(X^+) - f(X^-)$  for some function  $f$ , it is straightforward to solve the conservation equations. There are two inequivalent solutions,

$$\begin{aligned}
 \alpha : \quad & X^+ = Z^+ & X^+ &= Y^- \\
 & X^- = Y^+ & \beta : \quad & X^- = Z^- \\
 & Y^- = Z^- & & Y^+ = Z^+
 \end{aligned}
 \tag{15}$$

The two solutions are related by the interchange of  $X^\pm$  and  $Y^\pm$ .

Combining vertices of the type described above, we obtain the diagram shown in Figure 3a corresponding to the scattering of two BPS particles with spectral parameters  $X_1^\pm, X_2^\pm$ .

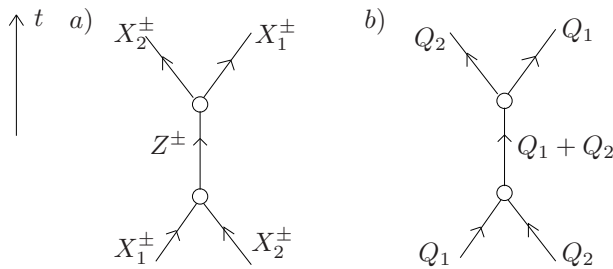


Figure 3: Formation of a bound state in the s-channel

If both particles belong to an  $SU(2)$  subsector they carry positive conserved charges  $Q_1 = n(X_1^\pm)$  and  $Q_2 = n(X_2^\pm)$ . The diagram corresponds to the formation of a BPS boundstate of charge  $Q_1 + Q_2$  in the s-channel. These charge assignments are shown in Figure 3b. For individual vertices the conservation laws can be implemented using either solution  $\alpha$  or  $\beta$  described above. However, once the vertices are connected by an internal line, consistency requires the choice of the same solution at both vertices. If we choose the solution  $\beta$  at both vertices, the spectral parameters of the internal line are fixed to be  $Z^+ = X_2^+$ ,  $Z^- = X_1^-$  and the diagram leads to an S-matrix pole when the parameters of the initial (and final) particles obey  $X_1^+ = X_2^-$ . This pole is present in (13). In addition, parametrizing the momenta as in (11) we find that  $q > 0$  at this pole. This can be seen most easily by noting that  $u_1 - u_2 = -i/g$  and that  $\partial_p u(p) < 0$  for real momenta. The other possibility is to choose the solution  $\alpha$  at each vertex which leads to the relation  $X_1^- = X_2^+$ . This possibility implies that  $q < 0$  and would not lead to bound states. The  $S$  matrix may or may not have a pole at this position, but we should not interpret it as a bound state. For example, in the  $SL(2)$  subsector there is a pole at this position, but we do not have boundstates associated with them.

The three-point vertices shown in Figure 2, are the only possible ones if all three particles belong to the same  $SU(2)$  sector. In any  $SU(2)$  sector, there is a conserved  $U(1)$  charge  $Q$  such that BPS particles of type  $n$  carry positive charge  $Q = n$ . However, the theory also contains BPS particles of negative charge  $Q = -n$  with respect to the same  $U(1)$ . The particles of negative charge correspond to a different  $SU(2)$  sector. For each value of  $n$ , the two particles belong to the same  $SU(2|2)^2$  multiplet, but have opposite charges under the Cartan generator corresponding to the  $U(1)$  in question. The crossing symmetry of the S-matrix suggests that we should also admit vertices for interactions between BPS particles of

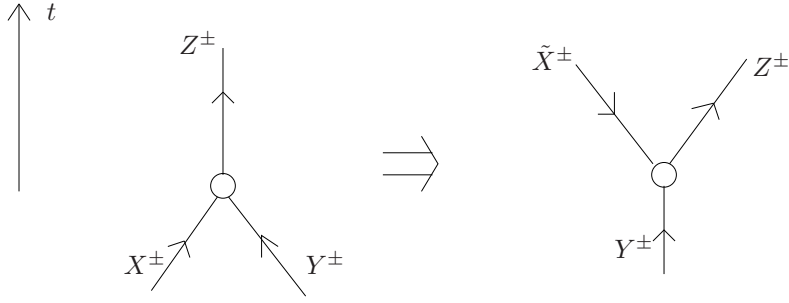


Figure 4: Crossing transformation of vertex.

positive and negative charge. For a BPS particle with spectral parameters  $X^\pm$  the crossing transformation is,

$$X^+ \rightarrow \tilde{X}^+ = 1/X^+ \quad X^- \rightarrow \tilde{X}^- = 1/X^- \quad (16)$$

This transformation changes the sign of the energy and momentum,  $E(\tilde{X}^\pm) = -E(X^\pm)$ ,  $p(\tilde{X}^\pm) = -p(X^\pm)$  but preserves the form of the constraint (4) with  $n(\tilde{X}^\pm) = n(X^\pm)$ . If we apply this transformation to a vertex with an *incoming* state of spectral parameters  $X^\pm$  and positive charge  $Q = n(X^\pm)$ , we obtain a new vertex with an *outgoing* particle of spectral parameters  $\tilde{X}^\pm$ . For the new vertex to conserve charge, we must interpret the outgoing particle as one of negative charge  $\tilde{Q} = -n(\tilde{X}^\pm) = -Q$ . We will indicate a particle of negative charge by reversing direction of the arrow appearing on its world line. To illustrate the crossing transformation we will apply it to an incoming leg on the vertex shown in Figure 2a to obtain a new vertex as shown in Figure 4. The solutions  $\alpha$  and  $\beta$  of the conservation laws for the original vertex yield two solutions for the new vertex,

$$\begin{aligned} \tilde{\alpha} : \quad & 1/\tilde{X}^+ = Z^+ & 1/\tilde{X}^+ = Y^- \\ & 1/\tilde{X}^- = Y^+ & 1/\tilde{X}^- = Z^- \\ & Y^- = Z^- & Y^+ = Z^+ \end{aligned} \quad (17)$$

A feature of these equations that is worth noting is the following. If particle  $Y^\pm$  is in the giant magnon regime, then one of the two other particles has to also be in the giant magnon regime while the last one is in the plane wave regime.

We can now discuss the pole at  $X_1^+ = 1/X_2^-$ . This arises naturally if we take the s-channel diagram and we cross one of the two particles. We then have a diagram that looks like the one in Figure 5 by using (17). Note that the intermediate particle has  $U(1)$  charge zero, but this

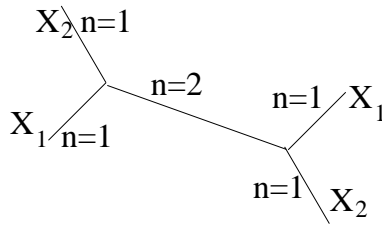


Figure 5: t-channel contribution

is not a problem since there are such particles in the full  $SU(2|2)^2$  multiplet corresponding to a BPS magnon with  $n = 2$ . When the external particles are in the near plane wave regime, it is clear that this is an allowed process since the theory is nearly relativistic.

If the external particles are both in the giant magnon region, then, as we mentioned after (17), the intermediate particle is in the plane wave regime. The two giant magnons behave as two heavy particles that are moving at slow relative velocities which are interacting through a potential generated by the exchange of the lighter particle. Let us now remind the reader how these poles arise when we think about the non-relativistic approximation for the two heavy particles. We will have a lagrangian of the form  $L \sim M\dot{x}^2 + e^{mx}$  where  $mx \ll 0$ . When we try to solve the problem in the Born approximation we are lead to

$$\mathcal{A} \sim \langle \Psi_{out} | V | \Psi_{in} \rangle = \int dx e^{-qx} e^{mx} e^{-qx} \quad (18)$$

which gives a divergence when  $q = m/2$ . Note that this divergence arises from long distance effects in the quantum mechanics problem and does not depend on the details of the potential at short distances. In addition, this feature is independent of the sign of  $M$ . Indeed, when we expand the giant magnon dispersion relation we will find that  $M$  is negative. The intermediate particle of mass  $m$  ( $m > 0$ ) is carrying momentum  $k \sim -im$ . In principle, one could have considered a situation where this particle carries momentum  $k \sim +im$ , but it would have given rise to an unphysical growing potential. We will use similar criteria in more complicated situations below in order to isolate the physical singularities from the unphysical ones. As we mentioned in Section 2, we can have singularities in unphysical sheets from such solutions.

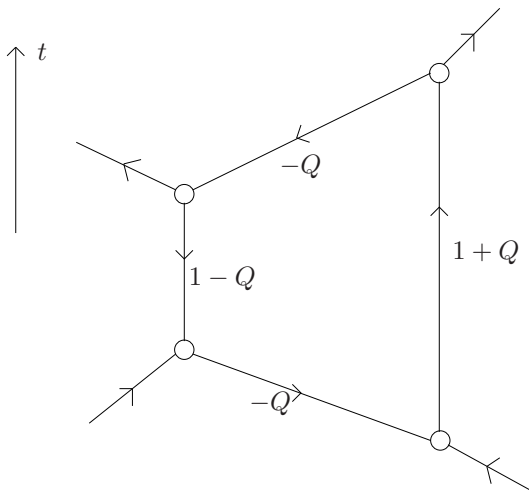


Figure 6: The box diagram.  $Q > 1$ .

### 3.2 Double poles

Following the discussion in Section 2, we look for diagrams that can give rise to double poles. Let us start by considering the one loop box diagram shown in Figure 6, where the external legs are all elementary magnons in the  $SU(2)$  sector and carry charge 1. The box diagram<sup>5</sup> represents an s-channel process where the intermediate states consist of two BPS particles of charges  $1 + Q$  and  $1 - Q$  where  $Q > 1$  is a positive integer. More generally the states going around the loop can correspond to other members of the corresponding BPS boundstate magnon multiplet which is labelled by the positive integer  $n$ . What will be important for us is the value of  $n$  for each of these magnons since it is the parameter appearing in the dispersion relation of the state. When we assign values of  $n$  for each of the internal lines we should remember that, since the external lines have  $n = 1$ , group theory says that at each vertex the values of  $n$  should differ by plus or minus one. In figure 7 we have written several choices. We will first concentrate on the one in figure 7a, which is the one suggested by figure 6. The choice in 7c gives the same condition as the one we will consider explicitly. The choices in 7b lead to inconsistent equations once we impose the condition that the pole is on the physical sheet.

To verify this is an allowed process there are two steps,

---

<sup>5</sup> This diagram is different from those considered by Coleman and Thun in the relativistic sine-Gordon case. In that case this diagram can also be considered and give singularities that coincide with the ones found in [15] using different diagrams.

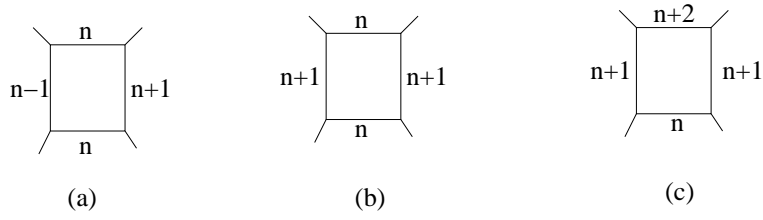


Figure 7: Several choices for the  $SU(2|2)^2$  representations appearing in the internal lines. In addition we can change the  $\pm 1$  to  $\mp 1$  to find new possibilities.

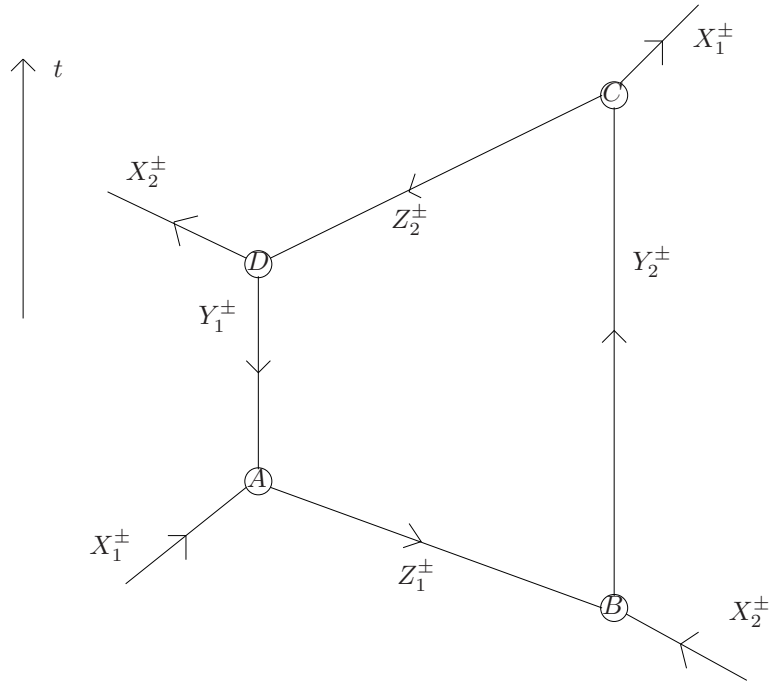


Figure 8: Spectral parameters and vertices for the box diagram.

- 1 Implement energy and momentum conservation at each vertex.
- 2 Impose additional conditions to make sure that the singularity arises on the physical branch.

We will find that after the first step, we will have fixed all the momenta of the intermediate lines, up to some discrete choices. The second condition will rule out some of them. In particular, we can perform approximations when we are evaluating the second condition, since the exact position of the poles is already fixed after the first step.

To perform the first step we assign spectral parameters to each line in the diagram as shown in Figure 8. Momentum and energy conservation are implemented by the vertex rules described above together with further rules obtained by repeated applications of the crossing transformation. There are two possible choices at each of the four vertices  $A$ ,  $B$ ,  $C$  and  $D$ . For each of these choices we will then have to evaluate the second criterion.

Let us first consider the case where the two particles are in the plane wave regime. There we can use the approximate relativistic formulas and demand that the graphs closes in “anti-Euclidean” space. Each of the vertices involves particles of mass 1 (the external line),  $Q$  and  $Q - 1$  (with  $Q > 1$ ). The solution to the energy and momentum conservation condition tells us that the momentum is approximately zero so that the energies are given approximately by 1 and  $Q$  and  $Q - 1$  respectively. Therefore the particles  $Q$  and  $Q - 1$  cannot be both be going into the future at this vertex. It is clear that we cannot obey this condition both at vertices  $A$  and  $B$ . Thus, none of the graphs gives rise to a singularity in the near plane wave region.

We now consider the case where both incoming particles are giant magnons. As we mentioned above, one of the particles emerging from the vertex has to be giant and the other a plane wave particle. Moreover, the giant particle has energy and momentum similar to the incoming particle. Thus, we expect that it continues to move to the future. Since the particle  $Z$  is coming from the past in vertex  $A$  or  $B$ , we conclude that particle  $Z$  must be of the plane wave type. Thus, we see that we have the qualitative conditions  $X_1^\pm \sim Y_1^\pm$  and  $Z^+ \sim Z^- = X_1^\pm$ , where the last sign will depend on the type of solution of the momentum conservation conditions (15) that we choose. For example, for vertex  $\mathbf{A}$  we have the two choices

$$\begin{array}{ll}
 X_1^+ = 1/Y_1^- & X_1^+ = 1/Z_1^+ \\
 \mathbf{A} : \quad X_1^- = 1/Z_1^- & \mathbf{A}' : \quad X_1^- = 1/Y_1^+ \\
 Y_1^+ = Z_1^+ & Y_1^- = Z_1^-
 \end{array} \tag{19}$$

Approximately, these two choices amount to saying whether  $Z \sim X_1^+$  (for  $\mathbf{A}$ ) or  $Z \sim X_1^-$  (for  $\mathbf{A}'$ ). For simplicity, let us analyze this condition around  $p = \pi$  (see (11)). Since this is a maximum in the dispersion relation we can go to “anti-Euclidean space” by setting  $p = \pi + iq$ . The expansion around this point looks similar to the non-relativistic expansion



of a relativistic theory, except for the sign of the mass. Moreover, we will have that  $q \ll 1$  and thus we will approximate  $X_1^+ \sim i$ ,  $X_2^- \sim -i$ . Equating these to  $Z$  and parametrizing its momentum as  $k = i\kappa$  (see (9)) we find that<sup>6</sup>

$$\mathbf{A} : \quad X_1^+ \sim Z_1, \quad \rightarrow i \sim \frac{n \pm \sqrt{n^2 - \kappa^2}}{i\kappa}, \quad \rightarrow \kappa \sim -n \quad (20)$$

$$\mathbf{A}' : \quad X_1^- \sim Z_1, \quad \rightarrow -i \sim \frac{n \pm \sqrt{n^2 - \kappa^2}}{i\kappa}, \quad \rightarrow \kappa \sim +n \quad (21)$$

As we mentioned above in our discussion of  $t$  channel contributions, we can interpret the exchange of the  $Z$  particle as giving rise to a potential which will go like  $e^{-\kappa x}$ . In order to get a sensible potential for  $x \ll 0$  we must demand that  $\kappa < 0$ . This selects the first condition, **A**.

This process can be repeated at each vertex and thus we select only one particular combination which is,

$$\begin{array}{ll} \mathbf{A} : & \begin{array}{l} X_1^- = 1/Z_1^- \\ Z_1^+ = Y_1^+ \\ Y_1^- = 1/X_1^+ \end{array} & \mathbf{B} : & \begin{array}{l} X_2^- = 1/Z_1^+ \\ X_2^+ = Y_2^+ \\ Y_2^- = 1/Z_1^- \end{array} \end{array} \quad (22)$$

$$\begin{array}{ll} \mathbf{C} : & \begin{array}{l} X_1^+ = 1/Z_2^- \\ 1/Z_2^+ = Y_2^+ \\ Y_2^- = X_1^- \end{array} & \mathbf{D} : & \begin{array}{l} Z_2^+ = 1/X_2^+ \\ Z_2^- = Y_1^- \\ 1/X_2^- = Y_1^+ \end{array} \end{array} \quad (23)$$

or, more simply,

$$\begin{array}{ll} X_1^+ = \frac{1}{Y_1^-} = \frac{1}{Z_2^-} & X_1^- = Y_2^- = \frac{1}{Z_1^-} \\ X_2^+ = Y_2^+ = \frac{1}{Z_2^+} & X_2^- = \frac{1}{Y_1^+} = \frac{1}{Z_1^+} \end{array} \quad (24)$$

From these relations as well as the constraints (4) on each set of spectral parameters we derive a condition on the rapidities of the two incoming particles,

$$u(X_1^\pm) - u(X_2^\pm) = -\frac{i}{g} n, \quad n > 1 \quad (25)$$

for each integer  $n > 1$ . In particular, the graph shown in Figure 6 gives rise to the double pole with  $n = Q$ . In Section 5 we will find that these are indeed the positions of the poles of the dressing factor  $\sigma^{-2}$ . Note that the other ways of solving the energy and momentum

---

<sup>6</sup>The choice of sign in the square root corresponds to the sign for the energy.

conservation conditions at each vertex, which we have ruled out by the arguments given above, would have led to equations similar to (25) but the integer in the right hand side would have had a different range.

We should note that when we write the condition of the pole as (25) we are losing some information since our analysis leading to (25) used that we were in the giant magnon region. Thus the condition (25) only applies in the giant magnon region where the real part,  $r_i$  of  $u_i$ , satisfies  $|r_i| < 2$ . On the other hand, we have already seen that in the plane wave region where  $|r_i| > 2$  there are no poles. Indeed, we will find that this is a feature of the proposed S-matrix in [1, 2].

### Other diagrams

In this section we will analyze other possible on-shell diagrams which might contribute. In particular we will consider diagrams of the type originally studied by Coleman and Thun [15] in the context of the sine-Gordon model. Since we have already accounted for all the poles in the  $S$  matrix, we expect that these diagrams give the same poles that we have found before. There are distinct graphs corresponding to s- and t-channel processes. A candidate t-channel diagram is shown in Figure 9. Relative to the process considered in the previous section, the new feature is that the internal legs cross in the center of the diagram and we must include the appropriate S-matrix element in our evaluation of the diagram. In the cases considered in [15], the central scattering process takes place at generic values of the momenta for which the corresponding S-matrix element is finite (and non-zero). In these cases, the extra factor is a harmless phase which does not affect the analysis of singularities. This needs to be reconsidered in the present case.

To verify the consistency of this diagram we will proceed exactly as in the previous subsection. First we assign spectral parameters to each internal line as shown in Figure 10. Conservation laws at each vertex are solved as follows,

$$\begin{array}{l}
 \mathbf{A} : \quad X_1^+ = 1/Y_1^- \quad X_2^+ = Z^+ \\
 \quad \quad X_1^- = Z^- \quad \mathbf{B} : X_2^- = 1/Y_2^+ \\
 \quad \quad 1/Y_1^+ = Z^+ \quad \quad \quad 1/Y_2^- = Z^-
 \end{array} \tag{26}$$

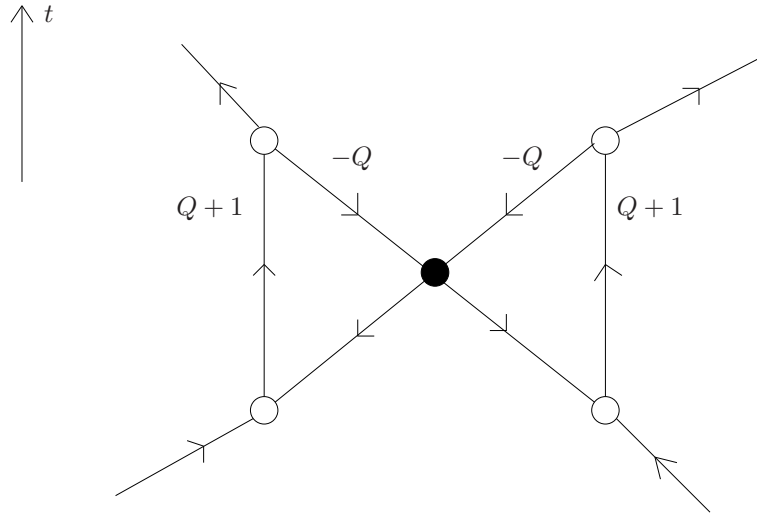


Figure 9: The spacetime graph for  $t$ -channel process.

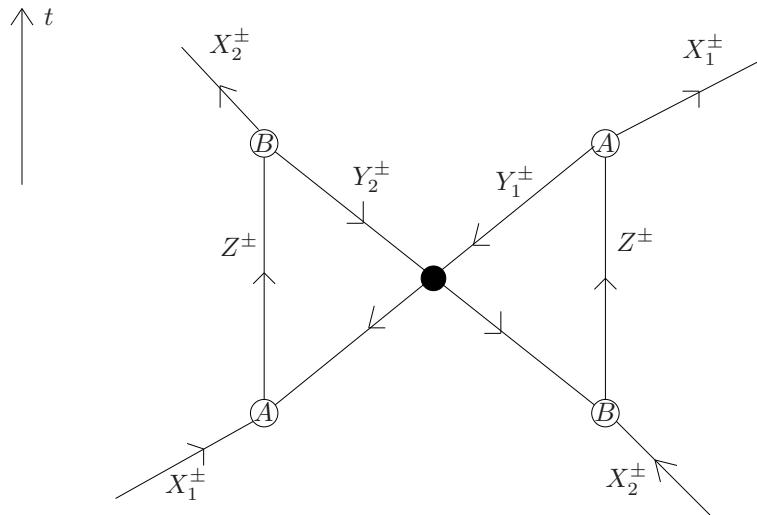


Figure 10: Spectral parameters and vertices for the  $t$ -channel diagram.

For the same reasons we discussed above this diagram does not lead to singularities if the external particles are in the plane wave region. Therefore, let us assume that the external particles are in the giant magnon region. As before there are other possible choices for the vertices but only this one is allowed, once we use the condition that the  $Y$  lines are in the plane wave region and that they should lead to reasonable potentials in the approximate quantum mechanics problem describing the slow motion of the particles. The relations (26) lead to the following condition on the rapidities of the incoming particles,

$$u_1 - u_2 = -\frac{i}{g} n, \quad n > 0 \quad (27)$$

where  $n = Q$  is a positive integer. Unlike the process considered in the previous subsection the case  $n = Q = 1$  is allowed.

Naively the above analysis predicts double poles at the positions given in equation (27). These coincide with the double poles we found earlier from the diagram in Figure 6 except for the case  $Q = 1$  which appears to predict a new double pole at  $X_1^+ = 1/X_2^-$ . However, we still have to consider the contribution of the “blob” in the centre of the diagram shown in Figures 10 and 9. In the case  $Q = 1$  this corresponds to the scattering of two anti-magnons with spectral parameters  $Y_1^\pm$  and  $Y_2^\pm$ . From the vertex conditions (26) we deduce that these parameters obey the relation  $Y_1^- = 1/Y_2^+$ . This is clearly a special value of the momentum. If the magnon  $S$  matrix has a pole of order  $D$  when  $X_1^+ = 1/X_2^-$  then, by unitarity, the  $S$ -matrix for two anti-magnons (which is the same as that for two magnons by crossing on both legs) will have a zero of degree  $D$  when the spectral parameters obey  $Y_1^- = 1/Y_2^+$ . Instead of simply predicting a double pole via the formula<sup>7</sup>

$$D = N - 2L = 6 - 4 = 2, \quad (28)$$

the Coleman-Thun analysis then yields a self-consistency equation for the degree  $D$  of the pole,

$$D = N - 2L - D = 2 - D \quad (29)$$

with solution  $D = 1$ . This indicates a *simple pole* at  $X_1^+ = 1/X_2^-$ . Thus this diagram gives also a simple pole. This is in agreement with the simple pole that we found from the  $t$  channel. It is also in agreement with the exact  $S$ -matrix where such a pole arises from the

---

<sup>7</sup>As above  $N$  is the number of internal lines and  $L$  is the number of loops in the diagram.

BDS contribution to the  $SU(2)$  sector S-matrix. In fact, similar considerations also hold for higher values of  $Q$  where the central scattering corresponds to a zero of the boundstate S-matrix obtained consistently by fusion [12]. In these cases the double zero cancels the double pole and the diagram is finite. Thus, we only obtain the single pole that is given by the  $t$  channel diagram.

## 4 Classical, semiclassical and approximate results

### 4.1 Localized classical solutions and the absence of non-BPS bound states

In a previous article by two of us [14], some localized oscillating solutions were found. There, it was proposed that these solutions could correspond to non-BPS bound states. As we have seen here, the singularities of the S-matrix are not interpreted as new particles, but come from physical processes involving the known BPS particles. In this section we discuss the solutions in [14] and explain why they do not give rise to bound states. What happens is that the “breather” solutions in [14] can be split into two BPS magnons with opposite charges. In order to see this, it is not enough to consider solutions in  $R \times S^2$  as it was done in [14], but one should consider solutions in a bigger subspace of  $AdS_5 \times S^5$ . It turns out that it is enough to consider solutions in  $R \times S^3$ . Solutions in this subspace were constructed by Spradlin and Volovich in [18] (see also [26] and appendix C ). Their solutions are functions of the worldsheet coordinates  $\sigma^{0,1}$  and of several complex parameters which we will denote<sup>8</sup> as  $\lambda_i^\pm$ . If we are to ensure that we have a proper real solution we generically need<sup>9</sup> that the complex conjugates of the set of parameters  $\{\lambda_i^+\}$  matches the set of parameters  $\{\lambda_i^-\}$ . The simplest solution corresponds to a BPS magnon of some charge. This solution is characterized by two parameters  $\lambda^\pm$  which are taken to be complex conjugates of each other. These parameters can be identified with the kinematic variables for the BPS magnon as  $X^\pm = \lambda^\pm$  when the conserved  $U(1)$  charge  $Q$  (denoted  $J_2$  in [18]) is positive. When this charge is negative the correct identification is  $X^+ = 1/\lambda^-$ ,  $X^- = 1/\lambda^+$

---

<sup>8</sup>They were called  $\lambda_i$  and  $\bar{\lambda}_i$  in [18]

<sup>9</sup>With the exception of the degenerate cases where the solution collapses to a single BPS soliton of charge  $Q$  (i.e.  $\lambda_1^- = \lambda_2^+$ ).

A second, more complicated solution was also considered in [18]. This solution depends on four complex parameters  $\lambda_1^\pm, \lambda_2^\pm$ . If we identify these parameters as the parameters of two magnons,  $X_i^\pm = \lambda_i^\pm$ , the solution describes the scattering of these two solitons. Also, if we take

$$\lambda_1^+ = 1/\lambda_1^-, \quad \lambda_2^+ = 1/\lambda_2^-, \quad (\lambda_1^+)^* = \lambda_2^-, \quad (\lambda_2^+)^* = \lambda_1^- \quad (30)$$

with a general complex value for  $\lambda_1^+$ , we recover the “breather” solution of [14]. Note that the solution depends on just one complex parameter which corresponds to the following two real variables: the momentum  $p$  of the breather and the excitation number  $\nu$ . This solution can be viewed as coming from the analytic continuation of the scattering of two zero charge magnons with rapidities  $X_i^\pm = \lambda_i^\pm$ . With this identification  $X_i^+ \neq (X_i^-)^*$ , so it seems we can’t view 1 and 2 as physical particles.

There is, however, a very interesting property of the solutions in [18]. They are symmetric under the exchange of the parameters  $\lambda_1^- \leftrightarrow \lambda_2^-$ , without exchanging<sup>10</sup> the parameters  $\lambda_i^+$ . Thus, we can take the “breather” solution we just mentioned and identify the rapidities of two magnons, instead, as

$$\begin{aligned} \lambda_1^+ &= X_1^+ & \lambda_2^+ &= X_2^+ \\ \lambda_1^- &= X_2^- & \lambda_2^- &= X_1^- \end{aligned}$$

We now see from (30) that  $X_i^+ = (X_i^-)^*$ . Therefore, the same solution can be viewed as arising from two magnons with kinematic variables corresponding to real physical variables of two BPS solitons with opposite charges, both moving with the same velocity. In this way we clearly see that the “breather” solution in [14] can be separated into a superposition of two physical particles<sup>11</sup>. Therefore, if we were to quantize the solution in [14] we would have a variable corresponding to the relative position of these two particles and we would not end up with a bound state.

As a side comment, the breather solutions in [14] for very high excitation number  $n = 2k + c$  (where  $c$  is a constant associated with the energy localized at the boundaries of the excitation

---

<sup>10</sup>Equivalently, we can exchange only  $\lambda_1^+ \leftrightarrow \lambda_2^+$ .

<sup>11</sup>The sine-Gordon theory also has localized oscillating solutions which do not correspond to new bound states, but are superpositions of the ordinary solitons and breathers (see [27] for example).

in (31) ) look like excitations of the form

$$\dots ZZZW\bar{Z}\dots\bar{Z}\bar{W}ZZZ\dots \quad (31)$$

where  $W$  and  $\bar{W}$  are two impurities and there are  $k$   $\bar{Z}$ s. This can split into two BPS magnon multiplet with charges  $n/2$  and  $-n/2$ , one made of  $n/2$   $W$ s and the other made of  $n/2$   $\bar{W}$ s.

In [18], another solution was considered which was called a “bound state” solution. It was constructed by performing an analytic continuation of the scattering solution for charged magnons. This solution also has rapidities related as  $\lambda_1^+ = (\lambda_2^-)^*$  and  $\lambda_1^- = (\lambda_2^+)^*$ . We see that under the exchange of the two  $\lambda_i^-$  we recover the kinematic variables of two physical magnons. Moreover, these two magnons have different velocities which implies that this “bound state” solution is simply an ordinary (non localized) scattering solution. It turns out, then, that all possible physical choices for the parameters  $\{\lambda_i^\pm\}$  yield a non-localized scattering solution<sup>12</sup>. Thus, we have concluded that there is no solution in the literature that looks like a (non-BPS) bound state. Therefore, there is no reason, from the classical solutions alone, to think there are more states in the spectrum than the BPS bound states.

This conclusion agrees with our picture from the analysis of poles in the previous section that already suggested that we should not be able to construct new non-BPS bound states, at least from the scattering of elementary magnons.

## 4.2 The semiclassical limit of the quantum theory

The processes considered in Section 3, leading to double poles at positions dictated by (25), can with be compared directly with the classical analysis. In the semiclassical limit,  $g \gg 1$ , the incoming particles correspond to Giant Magnons of charge<sup>13</sup>  $Q = 1 \sim 0$ . The corresponding classical solution has complex parameters  $X_i^\pm = \lambda_i^\pm$  where  $\lambda_i^\pm$  are related as in (30). On the other hand the intermediate state in the s-channel box diagram corresponds to two solitons of charges  $1 - Q \sim -Q$  and  $Q + 1 \sim Q$  with complex parameters,

$$\begin{aligned} \lambda_1^+ &= 1/Y_1^- & \lambda_2^+ &= Y_2^+ \\ \lambda_1^- &= 1/Y_1^+ & \lambda_2^- &= Y_2^- \end{aligned}$$

---

<sup>12</sup>With the exception, again, of some degenerate cases given by sets that collapse to the one particle BPS state of charge  $Q$  (i.e.  $\lambda_2^+ = \lambda_2^-$ ).

<sup>13</sup>By this we mean that the charge  $Q = 1$  carried by these states can be neglected in this limit.

which obey the reality conditions  $\lambda_1^+ = (\lambda_1^-)^*$  and  $\lambda_2^+ = (\lambda_2^-)^*$ . As the corresponding rapidities  $u(Y_1^\pm)$  and  $u(Y_2^\pm)$  vanish and both momenta are equal to  $\pi$ , both the constituent solitons are at rest. Note also that the particles of charge  $-Q$ , exchanged between the two massive solitons, have vanishingly small energy in the semiclassical limit.

The equalities (24) imply that the classical solutions corresponding to the incoming and intermediate states are related by the interchange of parameters,

$$\lambda_1^+ \rightarrow \lambda_1^+, \quad \lambda_2^+ \rightarrow \lambda_2^+, \quad \lambda_1^- \rightarrow \lambda_2^-, \quad \lambda_2^- \rightarrow \lambda_1^- \quad (32)$$

As this interchange is a symmetry of the two-soliton solution, the process corresponds to a *single* classical field configuration. This configuration can be interpreted as consisting of two solitons of opposite charge  $\pm Q$  which are both at rest or as consisting of two solitons of zero charge with complex momenta  $p_1 = \pi + iq$  and  $p_2 = \pi - iq$ . As already established, there is a space of such solutions with the sine-Gordon breather as a special case.

### 4.3 Scattering of giant magnons and a non-relativistic limit

If we consider a single magnon classical solution, as in [14], we find that the solution has fermionic and bosonic zero modes. These are also called “collective coordinates”. The bosonic zero modes parametrize the space  $R \times S^3$  where  $R$  denotes the position of the magnon and  $S^3$  parametrizes the orientation of the solution inside  $S^5$ . In addition we have fermion zero modes [28]. The quantization of all these zero modes should give the whole tower of BPS magnons. Suppose that we start with a given magnon of momentum  $\bar{p}$  and consider other magnons with very similar momentum. We can describe them by looking at the quantum mechanics of the collective coordinates. In order to understand what the Hamiltonian is we can expand the expression of the energy around a reference momentum<sup>14</sup>,  $p = \bar{p} + \frac{k}{2g}$ . Assuming  $0 < \bar{p} < 2\pi$

$$\begin{aligned} E &= \sqrt{n^2 + 16g^2 \sin^2 \frac{\bar{p}}{2}} = 4g \sin \frac{\bar{p}}{2} + \frac{1}{8g \sin \frac{\bar{p}}{2}} n^2 \\ &= \bar{E} + vk - \frac{1}{8g} \left| \sin \frac{\bar{p}}{2} \right| k^2 + \frac{1}{8g \left| \sin \frac{\bar{p}}{2} \right|} n^2 \end{aligned} \quad (33)$$

---

<sup>14</sup> In this normalization  $k$  is related to translations in the coordinate  $x$  introduced in (6). This is the normalization where the speed of light in the plane wave region is one.



with

$$v = \frac{dE}{dk} = \cos \frac{\bar{p}}{2} \quad \bar{E} = 4g \left| \sin \frac{\bar{p}}{2} \right| \quad (34)$$

As we saw above, diagrams giving rise to double poles involve “heavy” giant magnon particles and “light” plane wave particles. Double poles arise when two heavy particles exchange a pair of light particles. In this regime, where the relative motion of the heavy particles is slow, we expect that we should be able to view the problem as non-relativistic motion of the collective coordinates plus a potential that arises from the exchange of the light particles. Since the dispersion relation for the light particles is approximately relativistic the potential will have the usual Yukawa form for particles of mass  $m$ , i.e.  $V \sim e^{-mr}$  for  $mr \gg 1$ . However, we should recall that the two magnons are moving with similar velocities which are large,  $v_1 \sim v_2 \sim v$ . If we denote by  $x$  the distance between the two magnons, we find that the potential has the boosted form

$$V \sim \sum_n g f_n(\Omega_1, \Omega_2) e^{-n|x|\gamma}, \quad \gamma^{-2} = 1 - v^2 \quad (35)$$

where  $f_n$  is a function that depends on the angles on both  $S^3$ s and the fermion zero modes. We have also indicated how the potential scales with  $g$ . This scaling is determined as follows. We know that the classical solutions are independent of  $g$ . Thus, classical scattering properties, such as time delays are independent of  $g$ . Since the mass is proportional to  $g$  (see (33)), then, the potential should also be proportional to  $g$  such that the classical equations of motion are independent of  $g$ .

It is now convenient to rescale  $x \rightarrow \hat{x} = \gamma x$  and  $k \rightarrow \hat{k} = k/\gamma$ . We can also remove the linear term in the momentum in (33) by defining a new energy  $\hat{\epsilon}$  which is a linear combination of the old energy and the momentum,  $\hat{\epsilon} = \epsilon - vk$ . In these new variables we have a Hamiltonian

$$\hat{H} = \frac{1}{8g \left| \sin \frac{\bar{p}}{2} \right|} \left[ -\hat{k}_1^2 - \hat{k}_2^2 + n_1^2 + n_2^2 + \sum_n g^2 f_n(\Omega_1, \Omega_2) e^{-n|\hat{x}_1 - \hat{x}_2|} \right] \quad (36)$$

This is the form for the quantum mechanics of the collective coordinates in the slow relative velocity regime. We expect that the potential should be determined completely by the symmetries plus integrability, but we will not work it out here.

It is worth mentioning that, in these variables, the position of the double poles (see section 3) at  $u_1 - u_2 = -in/g$  is

$$\hat{k} = \frac{1}{2}(\hat{k}_1 - \hat{k}_2) = in, \quad \text{with } n = 2, 3, 4, \dots \quad (37)$$

where  $\hat{k}$  is the relative momentum conjugate to  $\hat{x}_1 - \hat{x}_2$ .

#### 4.4 A toy model for double poles

Since finding the full potential in (36) is beyond the scope of this paper we will consider a toy model which we can solve and is such that it also displays the double poles. Notice that in a non-relativistic quantum mechanics problem with one degree of freedom the scattering matrix can have only single poles [29]. In fact, in the quantum mechanical problem the poles can have different origins. We can have poles corresponding to bound states and we can have poles that arise because we have a potential decaying like  $e^{-mr}$  and there is a resonance between this exponential decay and the increase of the wavefunction as we discussed around (18). It should be emphasized that the pole originates from the tail of the potential and is independent of the details of the potential for small  $r$ . In the full relativistic theory, the bound states give rise to poles in the  $s$  channel and the tails of the potential to poles in the  $t$  channel.

The double poles we are considering also arise from the tails of the potential and are not related to bound states. In order to see them, we should include at least two degrees of freedom. We can include an internal angular coordinate  $\varphi$  which lives on a circle. If we have a potential of the form  $V \sim e^{in\varphi} e^{-m_n|x|}$ , then we will have double poles which can be interpreted, in a relativistic context, as coming from the exchange of a pair of massive particles.

In our toy model, instead of the full space of magnon collective coordinates, we will have  $R \times S^1$ . We denote by  $\varphi = \varphi_1 - \varphi_2$  the relative angular coordinate. We consider a theory where we only treat the relative coordinates  $x$  and  $\varphi$ . We now look for an integrable potential which contains the exchanged particles charged under the  $U(1)$  symmetry that shifts  $\varphi_i$ . We recall that the non-relativistic limit considered here has a counterpart in the sine-Gordon theory [17]. In that context, integrable potentials of the form  $V \sim \frac{1}{\sinh^2 x}$  arise. With this

in mind we can consider a simple generalization of this case that will fit our purposes. We propose to study the following hamiltonian

$$H = \frac{1}{2} \left[ -\hat{k}^2 + \ell^2 \right] + \frac{v}{4 \sinh^2 \left( \frac{\hat{x} + i\varphi}{2} \right)} + \frac{v}{4 \sinh^2 \left( \frac{\hat{x} - i\varphi}{2} \right)}, \quad v = \frac{1}{4} - \left( m + \frac{1}{2} \right)^2 \quad (38)$$

where  $v$  is a coupling constant (which we have parameterized in terms of another coupling  $m$ ),  $\hat{k}$  is the momentum conjugate to the relative coordinate and  $\ell$  is conjugate to  $\varphi = \varphi_1 - \varphi_2$ . As advertised, this model is integrable (for reviews on these Calogero-Sutherland systems see [30, 31, 32]), has the right classical limit and coupling dependence, as long as we make  $v \sim \mathcal{O}(g^2)$ . This system is naturally defined on the cylinder  $R \times S^1$ . Since we are considering the scattering of identical particles the space is really  $(R \times S^1)/\mathbb{Z}_2$ .

This potential is singular at  $z = 0$  and near the singularity it behaves as  $\cos(2\theta)/r^2$  where  $z = re^{i\theta}$ . Unfortunately, since the coupling constant is large, this means that the potential is attractive for some angles, and particles might “fall to the center”. This can be avoided by modifying the potential near the singularities. Since the poles we are interested in come from long distances, this should have no effect. We do not know of an easy way to modify the potential while preserving integrability. However, for particular values of the coupling  $v$  there exist explicit solutions of the above problem where the wavefunction vanishes at the singularities. Thus, a modification of the potential at the singularities to make the problem well defined should have no effect on these particular wave functions.

In order to solve this problem we define the following quantities

$$z = \frac{1}{2}(x + i\varphi) \quad \bar{z} = \frac{1}{2}(x - i\varphi) \quad (39)$$

$$\beta^2 + \bar{\beta}^2 = 4\hat{\epsilon} \quad \text{with} \quad H = \hat{\epsilon} = \frac{\ell^2}{2} - \frac{\hat{k}^2}{2} \quad (40)$$

Therefore the Schrodinger equation we need to solve is

$$\left[ \frac{\partial^2}{\partial z^2} - \beta^2 + \frac{v}{\sinh^2 z} \right] \psi = 0, \quad v = \frac{1}{4} - \left( m + \frac{1}{2} \right)^2 \quad (41)$$

and its barred version. Then, the general form of the solutions to this equation (and its bared version) are

$$\psi^\beta(z) = e^{\beta z} F(1 + m, -m, 1 - \beta, u) \quad \text{with} \quad u = \frac{1}{2} \left( 1 - \frac{1}{\tanh(z)} \right) \quad (42)$$

where  $F$  is the ordinary hypergeometric function  ${}_2F_1$ . The second independent solution is  $\psi^{-\beta}(z)$ . Therefore, the general form of the solutions to our whole problem is  $\Psi^{\beta, \bar{\beta}}(z, \bar{z}) = \psi^\beta(z)\psi^{\bar{\beta}}(\bar{z})$  with  $\beta, \bar{\beta}$  satisfying (40). We can check that in the large  $x$  region the wave function behaves as

$$\Psi^{\beta, \bar{\beta}}(z, \bar{z}) \sim e^{\beta z + \bar{\beta} \bar{z}} \sim e^{i\hat{k}x + i\ell\varphi}, \quad x \gg 0, \quad \beta = \ell + i\hat{k}, \quad \bar{\beta} = -\ell + i\hat{k} \quad (43)$$

where  $\ell$  is integer, since  $\varphi$  is periodic. One important condition is that the wave function remains normalizable in the neighborhood of the singularity located at  $z = \bar{z} = 0$ . In fact, we see that two independent solutions of (41) go like  $z^{-m}$  and  $z^{1+m}$ . Let us assume that  $m$  in integer<sup>15</sup>. We then see that if we demand that the wavefunction is antisymmetric<sup>16</sup> under  $z \rightarrow -z$  and  $\bar{z} \rightarrow -\bar{z}$  we need to combine solutions so that we have combinations such as  $z^{-m}\bar{z}^{1+m}$  and  $z^{1+m}\bar{z}^{-m}$  near the origin. We see that such combinations vanish as we approach  $z \rightarrow 0$  so that a small modification of the potential is not expected to affect the solutions in an important way. In terms of the functions (43) we need to consider the following combination

$$\Psi(z, \bar{z}) = -\Psi(-z, -\bar{z}) = \frac{\Gamma(1+m-\beta)\Gamma(1+m-\bar{\beta})}{\Gamma(1-\beta)\Gamma(1-\bar{\beta})}\Psi^{\beta, \bar{\beta}} - \frac{\Gamma(1+m+\beta)\Gamma(1+m+\bar{\beta})}{\Gamma(1+\beta)\Gamma(1+\bar{\beta})}\Psi^{-\beta, -\bar{\beta}} \quad (44)$$

The fact that the wavefunction is antisymmetric suggests that it is a natural solution to the problem of scattering of identical fermions, rather than bosons. Using the asymptotic expression (43), we can read off the S-matrix of this problem from the coefficients in (44) to be

$$S(\beta, \bar{\beta}) = -\frac{\Gamma(1+m-\beta)\Gamma(1+m-\bar{\beta})}{\Gamma(1-\beta)\Gamma(1-\bar{\beta})} \frac{\Gamma(1+\beta)\Gamma(1+\bar{\beta})}{\Gamma(1+m+\beta)\Gamma(1+m+\bar{\beta})}$$

If we scatter particles 1 and 2 with equal angular momentum  $J_2$ , then the relative angular momentum vanishes,  $\ell = 0$  and  $\beta = \bar{\beta} = i\hat{k}$ . In this situation the S-matrix is

$$S = -\frac{(1-i\hat{k})^2(2-i\hat{k})^2(3-i\hat{k})^2\dots(m-i\hat{k})^2}{(1+i\hat{k})^2(2+i\hat{k})^2(3+i\hat{k})^2\dots(m+i\hat{k})^2} \quad (45)$$

---

<sup>15</sup> Curiously, for integer  $m$ , these models naturally arise from matrix quantum mechanics [32]. At these values of the coupling the potential  $1/\cosh^2 z$  is also reflectionless. We also see that (43) becomes an order  $m$  polynomial of  $u$ .

<sup>16</sup>We actually need wavefunctions that have definite parity. It turns out that symmetric ones have a singular behavior at the singularity, so we need to consider antisymmetric ones. Actually, there is a physical interpretation of why only antisymmetric functions survive. As the interaction has a  $\cos 2\theta$  term near the origin, only odd angular momentum states are such that the potential averages to zero over an orbit. Symmetric states, thus, fall to the center.

This expression has double poles at  $\hat{k} = in$  with  $n = 1, 2, 3, \dots, m$ . We discussed in the last subsection that, from dynamical arguments, the coupling of the quantum mechanical model for the collective coordinates needs to be of order  $\mathcal{O}(g^2)$ . Therefore we need  $m \sim \mathcal{O}(g)$ . In the large  $g$  regime we obtain the infinite series of double poles that we expected from the complete theory. However, we also obtain an extra double pole at  $\hat{k} = i$ . This is not unexpected as our toy model does not forbid  $J_2 = 0$  states for the heavy particles<sup>17</sup>. Note that there is no single pole related to the fact that, in the toy model, the exchanged particles change  $\ell$ . In the true theory there is a single pole at  $\hat{k} = i$ . On the other hand if we look at the S-matrix for  $\ell \neq 0$  we find a simple pole at  $\hat{k} = i|\ell|$  representing the t-channel exchange of the particle that is giving rise to the potential in the toy model. In this case, we also retain double poles for  $\hat{k} = ir$  with  $r = 1 + |\ell|, 2 + |\ell|, \dots$

We conclude that this very simple model presents many of the characteristics associated with the complete S-matrix of the full string theory. Of course, it would be nice to find the correct quantum mechanics theory that describes the full problem in this regime.

## 5 Poles in the Beisert-Eden-Hernandez-Lopez-Staudacher S-matrix

### 5.1 Integral expression for the dressing factor

In [1, 2] a conjecture was made for the exact form of the unknown dressing factor that appears in the magnon S-matrix. This dressing factor was expressed as

$$\sigma^2 = \frac{R^2(x_1^+, x_2^+)R^2(x_1^-, x_2^-)}{R^2(x_1^+, x_2^-)R^2(x_1^-, x_2^+)}, \quad R^2(x_1, x_2) = e^{i2\chi(x_1, x_2) - i2\chi(x_2, x_1)} \quad (46)$$

The function  $\chi$  was given as a series expansion in powers of  $1/x_i$ . In order to study its analytic structure it is more convenient to write it as an integral expression. We find it convenient to introduce a new function  $\tilde{\chi}(1, 2)$ , which differs from  $\chi(1, 2)$  in [2] by terms that are symmetric under  $1 \leftrightarrow 2$ . Such symmetric terms cancel in (46) and thus  $\tilde{\chi}$  will lead to the same dressing factor if we use it in (46). In appendix A we derive the following

---

<sup>17</sup>Note, however, that they are indeed excluded for the intermediate ‘‘light’’ states. This can be seen by expanding the effective potential at large distances.

integral expression for  $\tilde{\chi}$  from the formulae in [2]

$$\tilde{\chi}(1, 2) = -i \oint \frac{dz_1}{2\pi} \oint \frac{dz_2}{2\pi} \frac{1}{(x_1 - z_1)(x_2 - z_2)} \times \log \Gamma\left(1 + ig\left(z_1 + \frac{1}{z_1} - z_2 - \frac{1}{z_2}\right)\right) \quad (47)$$

where the integral is over the contours with  $|z_1| = |z_2| = 1$ . With these contours the integral is well defined and there are no singularities on the integration contour if we assume that  $|x_1|, |x_2| > 1$ , as it is the case for physical particles.

## 5.2 Poles of the dressing factor in the giant magnon region

As we start analytically continuing in  $x_1$  and  $x_2$  we might encounter singularities. Singularities will appear when poles or branch cuts of the integrand pinch the contour. We will study only a subset of all possible singularities. We will set  $g$  to be large and then we will focus on the giant magnon region with fixed  $p$ , there  $x^\pm$  are near the unit circle but away from  $x^\pm = 1$ . We will then analytically continue away from physical values of  $x^\pm$  in this region, but we will still stay near the unit circle and far from  $x^\pm = 1$ . In other words, starting from the original values for  $p_1$  and  $p_2$  we will analytically continue only in a small neighborhood of these values of order  $1/g$  around the physical values.

In order to find the poles of  $\tilde{\chi}$  in (47), we view it as a function of three independent variables:  $g$ ,  $x_1$  and  $x_2$ . In order to avoid having to keep track of the branch of the log in (47) we take a derivative of  $\tilde{\chi}$  with respect to  $g$ . This will allow us to isolate the singularities of  $\tilde{\chi}$  that depend on  $g$ . In fact, there are no singularities that are independent of  $g$  because we can set  $g = 0$  and we see that  $\tilde{\chi}$  is identically zero. Thus, taking the derivative and disregarding some terms that do not contribute to the integral we find

$$\begin{aligned} g^2 \partial_g \tilde{\chi} &= \sum_{n=1}^{\infty} g^2 \partial_g \tilde{\chi}_n \\ g^2 \partial_g \tilde{\chi}_n &= - \oint \frac{dz_1}{2\pi} \frac{dz_2}{2\pi} \frac{1}{(x_1 - z_1)(x_2 - z_2)} \times \frac{n}{-i\frac{n}{g} + z_1 + \frac{1}{z_1} - z_2 - \frac{1}{z_2}} \end{aligned} \quad (48)$$

We now do the integral over  $z_1$  by deforming the contour, which starts out at  $|z_1| = 1$ , towards the origin of the  $z_1$  plane. The only poles we find come from the last factor in (48). The pole is at  $z_1 = z_n(z_2)$  where the function  $z_n(z)$  is defined as the solution to

$$z_n + \frac{1}{z_n} - z - \frac{1}{z} = i\frac{n}{g}, \quad n > 0 \quad (49)$$

as in [1]. Out of the two roots of this equation we should pick out the root whose absolute value is less than one. We can select this root unambiguously if  $|z| = 1$ . So from now on we only talk about this root and its analytic continuation as a function of  $z$ . We thus find that the result of the  $z_1$  integral is

$$g^2 \partial_g \tilde{\chi}^n = -i \oint \frac{dz}{2\pi} \frac{1}{(x_2 - z)(x_1 - z_n(z))} \times \frac{n}{1 - \frac{1}{z_n^2(z)}} \quad (50)$$

where we have set  $z = z_2$ .

We would like to understand where (50) has poles when we change  $x_i$ . Note that if  $|x_i| > 1$  (at it is the case for physical values) then the integral is finite. As we start analytically continuing  $x_i$  we could have a situation where the pole at  $z_2 = x_2$  moves inside the unit circle. In that case, we might think that all we need to do is to deform the contour so that  $|z_2| < 1$ , but this could push  $z_n(z_2)$  to larger values in such a way that it becomes equal to  $x_1$ . In other words, there is pole only if two poles of the integrand pinch the integration contour. We discuss below when this happens. If the contour is indeed pinched then the integral is equal to  $-2\pi i$  times the residue at  $z_2 = x_2$ . This gives

$$\begin{aligned} g^2 \partial_g \tilde{\chi}^n &= -\frac{1}{x_1 - x_n(x_2)} \frac{n}{1 - \frac{1}{x_n^2(x_2)}} \\ \tilde{\chi} &= -i \log(x_1 - x_n(x_2)) \end{aligned} \quad (51)$$

We then find that  $e^{2i\tilde{\chi}} \sim (x_1 - x_n(x_2))^2$  has double zeros.

### 5.3 When do we pinch the contour?

We need to understand some aspects of the function  $z_n$  more precisely (see Figure 11). The essential feature is the following. If we set  $z = e^{i\theta}$  then  $z_n \sim 1/z$  for  $0 < \theta < \pi$  and  $z_n \sim z$  for  $-\pi < \theta < 0$ . Recall also that in the giant magnon region the physical values of  $x^\pm \sim e^{\pm ip/2}$ . Both are close to the unit circle but  $x^+$  is in the upper half plane and  $x^-$  in the lower half plane.

Suppose that we have  $x_2 = x_2^+$ . This will be on the upper half plane and for finite and physical (real) values of  $p_2$  it will be close to the unit circle, but outside the unit circle. If we keep  $x_1$  fixed and we analytically continue in  $x_2^+$  then we see that  $z_n$  will be in the lower half plane when  $z \sim x_2^+$ , thus we can only pinch the contour if  $x_1$  is also in the lower half

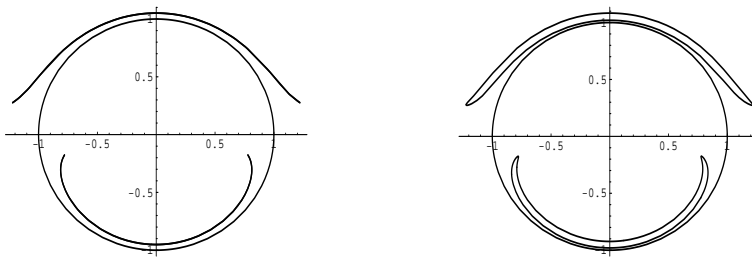


Figure 11: On the left we see plots of  $z_n(z)$  and  $1/z_n(z)$  for  $z$  on the unit circle. The circle gets mapped to an interval.  $z_n$  is the one inside the unit circle. We have set  $n/g = 0.1$ . In the plot on the right we have taken  $|z| = .98 < 1$ .

plane. This happens when  $x_1 = x_1^-$ , but not for  $x_1 = x_1^+$ . Since  $z_n \sim 1/z$  for  $z \sim x_2^+$  we find that  $|z_n|$  increases as  $|z|$  decreases (see Figure 11). Thus we pinch the contour when  $x_2 = x_2^+$  and  $x_1 = x_1^-$ .

Now suppose that  $x_2 = x_2^-$ . If  $z \sim x_2^-$  we have  $z_n \sim z$  so that when we decrease  $|z|$  we will also decrease  $|z_n|$  and we will not pinch the contour. So the only case where we pinch the contour is when  $x_2^+ = z$  and  $x_1^- = z_n$ . Of course, we have discussed poles from  $\tilde{\chi}(1, 2)$ . When we consider  $\tilde{\chi}(2, 1)$  we have the same story with  $1 \leftrightarrow 2$ .

Thus, the final result is that we have poles and zeros of the form

$$\sigma^2 \sim e^{-2i(\tilde{\chi}(x_1^-, x_2^+) - \tilde{\chi}(x_2^-, x_1^+))} \sim \prod_{n>0} \frac{(x_2^- - x_n(x_1^+))^2}{(x_1^- - x_n(x_2^+))^2} \quad (52)$$

We have only indicated terms that give rise to poles or zeros in the region of interest (large  $g$ ,  $p_1 \sim p_2$  of order one and  $p_1 - p_2 \sim \mathcal{O}(g)$ ). Of course, the expression for the location of poles is exact and we will find poles at these locations in the appropriate branch for any values of  $p_i$  and  $g$ .<sup>18</sup>

The double zeros of  $\sigma^2$  (or double poles of  $\sigma^{-2}$ ) lie at

$$x_2^- = x_n(x_1^+), \quad n > 0 \quad (53)$$

This implies that

$$u_1 - u_2 = -\frac{i(n+1)}{g} = -i\frac{m}{g}, \quad m > 1 \quad (54)$$

---

<sup>18</sup> Note that there are not poles or zeros at  $x_1^- = x_n(x_2^-)$  in the branch describing the neighborhood of the giant magnon region. Such poles are probably present on another branch.



Thus we see that the poles do not start at one. In fact, we do not get poles in  $\sigma^{-2}$  for  $m = 1$ .<sup>19</sup> Note that equation (53) contains more information than (54) since we have specified a particular branch of the function  $x_n$ . In fact, if we only looked at (54) we might incorrectly conclude that there are poles in the near plane wave region with  $x_1^\pm \sim x_2^\pm$  and  $|x_i^\pm| \gg 1$ . On the other hand, we see from (53) that in this region  $x_n(x_1^+) \sim 1/x_1^+$ , whose absolute value is not much larger than one. Of course, it is obvious from the integral expression (47) that there are no poles in the region  $|x_i| > 1$  since the integral is explicitly finite there.

In this whole discussion we have assumed that  $n \ll g$ . If this were not the case, we would have to move by a larger amount from the giant magnon region and we would have to understand better the whole analytic structure of the function. Finally we note that a related integral representation of the BHL/BES phase has recently been obtained in [34]. Like Eqn (48) above, the formula (5.11) appearing in this reference is also suggestive of a sum over intermediate states involving BPS particles.

## 6 Conclusions

We have understood the physical origin of the poles in the S matrix for the scattering of fundamental magnons. These poles can be cleanly isolated for strong coupling in the giant magnon region. In this case, the poles are far from other singularities of the S matrix. These poles can be explained by the interchange of BPS magnons. The origin of the double poles in the magnon S-matrix is the same as the origin of the double poles in the sine Gordon S-matrix. The position of the poles is determined by the spectrum of BPS particles of the model. These poles are accounted for by considering all the BPS particles that were found to exist on this chain. Therefore there is no reason to think that the spin chain has any other bound states beyond the BPS ones we already know about. In fact, the localized non-BPS classical solutions that were found in [14] were shown to be continuously connected to separated BPS magnon configurations. Thus, those solutions do not correspond to new states. One thing that we have not explored is the physical origin of the branch cuts in the dressing factor. It would be very nice to understand these more precisely.

---

<sup>19</sup> Notice, however, that there are poles (or zeros) at that position in the one loop factor answer in [1] (see also [33]). These poles (or zeros) are cancelled by all the higher order contributions.

ND is supported by a PPARC Senior Fellowship. JM was supported in part by DOE grant #DE-FG02-90ER40542.

## A Derivation of (47)

We start from the expression for  $\chi(x_1, x_2)$  as in equation (A.9) of [2]

$$\begin{aligned}\chi &= -2 \sum_{r=2}^{\infty} \sum_{s=r+1}^{\infty} \cos\left(\frac{\pi}{2}(s-r-1)\right) \frac{1}{x_1^{r-1} x_2^{s-1}} \int_0^{\infty} \frac{dt}{t} \frac{J_{r-1}(2gt) J_{s-1}(2gt)}{e^t - 1} \\ \chi &= -2 \frac{1}{x_1 x_2^2} \sum_{w=0}^{\infty} \sum_{l=0}^{\infty} (-1)^l \frac{1}{(x_1 x_2)^w x_2^{2l}} \int_0^{\infty} \frac{dt}{t} \frac{J_{w+1}(2gt) J_{2+2l}(2gt)}{e^t - 1}\end{aligned}\quad (55)$$

where  $s = r + 1 + 2l$  and  $r = w + 2$ . We then use the following expression for the Bessel functions

$$J_n(z) = \int_0^{2\pi} \frac{d\theta}{2\pi} e^{-in\theta + iz \sin \theta} \quad (56)$$

We insert these expressions in the above formulas, we perform the sums and after a simple shift of the integration variables we obtain

$$\begin{aligned}\chi &= 2i \frac{1}{x_1 x_2^2} \int_0^{2\pi} \frac{d\theta_1}{2\pi} \int_0^{2\pi} \frac{d\theta_2}{2\pi} e^{-i\theta_1 - 2i\theta_2} \frac{1}{\left(1 - \frac{e^{-2i\theta_2}}{x_2^2}\right) \left(1 - \frac{e^{-i\theta_1 - i\theta_2}}{x_1 x_2}\right)} \times \\ &\quad \times \int_0^{\infty} \frac{dt}{t} \frac{e^{i(2gt)(-\cos \theta_1 + \cos \theta_2)}}{e^t - 1}\end{aligned}\quad (57)$$

We now use that

$$\int_0^{\infty} \frac{dt}{t} \frac{e^{-zt}}{e^t - 1} = C_1 + zC_2 + \log \Gamma(1 + z) \quad (58)$$

where  $C_1$  and  $C_2$  are divergent constants which do not contribute once we do the integral over  $\theta_i$ . We then find

$$\begin{aligned}\chi &= 2i \frac{1}{x_1 x_2^2} \int_0^{2\pi} \frac{d\theta_1}{2\pi} \int_0^{2\pi} \frac{d\theta_2}{2\pi} e^{-i\theta_1 - 2i\theta_2} \frac{1}{\left(1 - \frac{e^{-2i\theta_2}}{x_2^2}\right) \left(1 - \frac{e^{-i\theta_1 - i\theta_2}}{x_1 x_2}\right)} \times \\ &\quad \times \log \Gamma(1 + i2g(\cos \theta_1 - \cos \theta_2))\end{aligned}\quad (59)$$

This last term looks a bit messy and with many possible branch cuts.

Let us simplify this expression a bit more. First we note that we can write (59) as

$$\begin{aligned}
\chi &= \int \frac{2e^{-i\theta_2}}{x_2} \frac{1}{1 - \frac{e^{-i2\theta_2}}{x_2^2}} f(\theta_1, \theta_2) \\
&= \int \left[ \frac{1}{1 - \frac{e^{-i\theta_2}}{x_2}} - \frac{1}{1 + \frac{e^{-i\theta_2}}{x_2}} \right] f(\theta_1, \theta_2) \\
&= \int \frac{1}{1 - \frac{e^{-i\theta_2}}{x_2}} [f(\theta_1, \theta_2) - f(\theta_2, \theta_1)] \\
&= \int \left[ \frac{1}{1 - \frac{e^{-i\theta_2}}{x_2}} - \frac{1}{1 - \frac{e^{-i\theta_1}}{x_2}} \right] f(\theta_1, \theta_2)
\end{aligned} \tag{60}$$

where we used that  $f(\theta_1 + \pi, \theta_2 + \pi) = f(\theta_2, \theta_1)$ . We have also relabelled the integration variables.

By forming the antisymmetric combination  $\chi_a(1, 2) \equiv \chi(1, 2) - \chi(2, 1)$  it is possible to simplify this expression further. One can see that

$$\begin{aligned}
\chi_a(1, 2) &= i \int \frac{d\theta_1}{2\pi} \frac{d\theta_2}{2\pi} e^{-i\theta_1 - i\theta_2} \frac{(x_1 - x_2)(e^{-i\theta_2} - e^{-i\theta_1})}{(x_1 - e^{-i\theta_1})(x_2 - e^{-i\theta_2})(x_1 - e^{-i\theta_2})(x_2 - e^{-i\theta_1})} \times \\
&\quad \log \Gamma(1 + i2g(\cos \theta_1 - \cos \theta_2)) \\
&= -i \oint \frac{dz_1}{2\pi} \frac{dz_2}{2\pi} \frac{(x_1 - x_2)(z_2 - z_1)}{(x_1 - z_1)(x_2 - z_2)(x_1 - z_2)(x_2 - z_1)} \times \\
&\quad \log \Gamma(1 + i2g(\cos \theta_1 - \cos \theta_2)) \\
&= -i \oint \frac{dz_1}{2\pi} \oint \frac{dz_2}{2\pi} \left( \frac{1}{(x_1 - z_1)(x_2 - z_2)} - \frac{1}{(x_1 - z_2)(x_2 - z_1)} \right) \times \\
&\quad \times \log \Gamma(1 + i2g(\cos \theta_1 - \cos \theta_2))
\end{aligned} \tag{61}$$

where we have set  $z_i = e^{-i\theta_i}$ . In these expressions, of course, we replace  $2 \cos \theta_1 = z_1 + \frac{1}{z_1}$ , etc. Note that we can view this last expression as arising from  $\chi_a(1, 2) = \tilde{\chi}(1, 2) - \tilde{\chi}(1, 2)$  with  $\tilde{\chi}$  as in (47), which is the formula we wanted to derive.

## B Diagrammatic form of the conservation equations in section 3

In order to write all, a priori, possible diagrams that lead to physical processes it is useful to adopt a diagrammatic form that matches each set of equation one to one. If we consider a general interaction vertex (given by the solutions to the conservation equations (14)) we see that all possible situations (where the quantum numbers  $n$  are considered free) arise from

crossing transformations of the vertices labeled  $\alpha$  and  $\beta$ . In total, there are six possibilities for each graph, giving a total number of 12 vertices (of course, for given incoming and outgoing particles of fixed  $n$  there will always be two possibilities). A convenient representation is a double line notation for each state, where each line joining spectral parameters represents an equality. If we follow a pair of lines forward in time the right line always represents  $X^+$  while the left one represents  $X^-$ . We also allow these lines to twist (cross), representing interchange of  $+ \leftrightarrow -$  and (as it will be convenient to consider crossing) inversion. That is, if two spectral parameters, say  $X^+$  and  $Y^+$  are connected, then  $X^+ = (Y^+)^{(-1)^k}$ , where  $k$  is the number of times that line crossed other lines. In particular, the vertices  $\alpha$  and  $\beta$  are given by

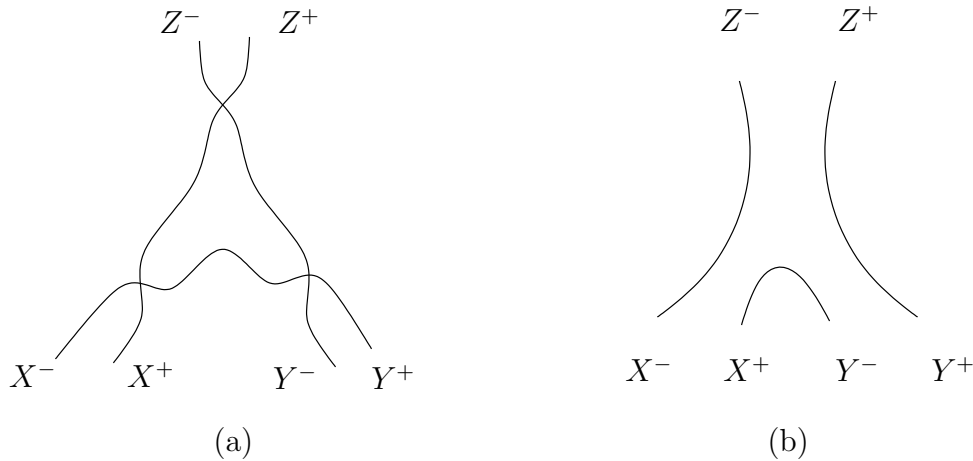


Figure 12: These are the vertices  $\alpha$  (a) and  $\beta$  (b) described in section 3. Each magnon is represented by a double line (a “string”) that is allowed to twist. Notice that since all lines cross other lines twice there is no inversion to consider. Using crossing symmetry we can obtain all other diagrams.

Since one wants to draw complicated diagrams (like the ones in section 3), the double line notation might get confusing. An economic way of representing the same information is to consider single line diagrams, where the single line separates  $+$  from  $-$ . We add a dot on top of the single line, near the vertex, when that “string” is twisted. In this simple way, applying crossing symmetry is just adding a dot (or suppressing it) and move the particle from the past to the future (or viceversa). In this way we can present all possible vertices as:

From these building blocks we can construct any complicated diagram. Notice that

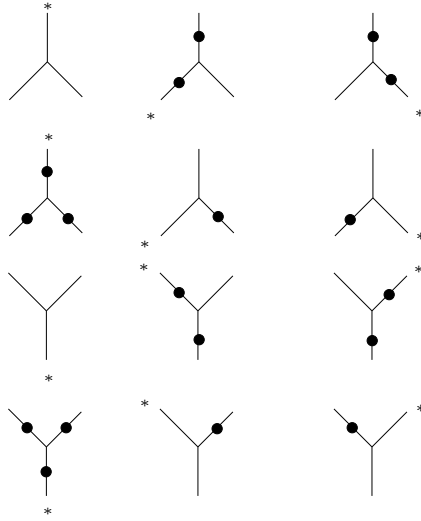


Figure 13: These are all possible vertices in single line notation. Vertex  $\beta$  is the first in the first line, while  $\alpha$  is the first in the second line. All other vertices come from applying crossing to these two. Notice, also, that lines 2 and 4 are obtained from 1 and 3 by just adding dots where there was none and suppressing them where there used to be one. This amounts to changing  $+ \leftrightarrow -$ . Finally the  $*$  marks the leg that carries the higher charge  $n_1 + n_2$ , as all vertices that we consider join charges,  $n_1$ ,  $n_2$  and  $n_1 + n_2$ . As promised there is only two vertices (related by  $+ \leftrightarrow -$ ) for a given structure of  $n$ 's.

although there are 12 vertices, there are only 6 types of equations in each vertex (2 for every  $n$  structure). That means that we can only think of vertices when two particles come from the past and one goes to the future (the first six in figure 13). The others just represent the same equations (lines 2 and 3 are equivalent as are 1 and 4 in the same figure).

If we have a fixed structure for the  $n$ 's carried by each line in the graph (as in the analysis of section 3), we only have to be careful about the  $*$ 's in the vertices (see caption of figure 13). One nice feature of this notation is that if we are only interested in equations relating the spectral parameters of external lines we can “detach” the dots from the vertices and assign them to propagators. If a propagator ends up with two dots, from both neighboring vertices, they just cancel each other. Once this is done it is very simple to read the equations from the diagram by following the parameters along the lines, remembering that dots interchange  $+$  and  $-$  and that the final equation contains an inverse if we went through an odd number of dots.

There are a number of rules one can derive from these graphs. For example, if all external

particles have  $n = 1$ , then the number of dots in the internal propagators of a box diagram is even. This is a consequence of the fact that a box diagram always has two  $2 \rightarrow 1$  vertices and two  $1 \rightarrow 2$  vertices. Notice also that  $n$  has to go back to itself after going around the loop. That also means that we have to have two vertices that increase  $n$  and two that decrease  $n$ .

Let us work out an example explicitly. The box diagram that was discussed in detail in section 3 (figure 6) can be drawn in this notation as

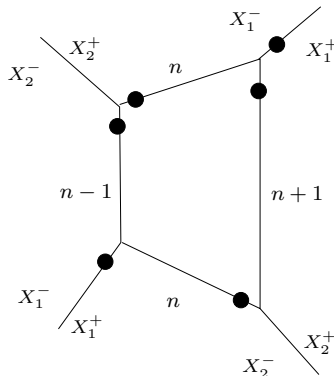


Figure 14: This is the “dotted” version of figure 6 in section 3.

It is easy to read from this picture that the outer spectral parameters just get mapped to themselves. The only constraint comes from the “mass” equation (4) for the propagators in the box. From analyzing one of the propagators, for example the bottom one, we see that this is just

$$\left(X_2^- + \frac{1}{X_2^-}\right) - \left(X_1^- + \frac{1}{X_1^-}\right) = \frac{in}{g} \quad (62)$$

which leads to the condition obtained for the double pole in section 3.

## C Classical magnon solutions found by Spradlin and Volovich [18]

For the reader’s convenience we reproduce the solutions in [18]. We will use complex target space coordinates  $Z_1 = X_1 + iX_2$  and  $Z_2 = X_3 + iX_4$  describing an  $S^3$  given by  $|Z_1|^2 + |Z_2|^2 = 1$ . The one magnon solution, written in terms of the  $\lambda^\pm$  and worldsheet  $\sigma^{0,1}$  variables, is

given by

$$Z_1 = \frac{e^{+i\sigma^0}}{\sqrt{\lambda^+\lambda^-}} \frac{\lambda^+ e^{-2iZ^+} + \lambda^- e^{-2iZ^-}}{e^{-2iZ^+} + e^{-2iZ^-}} \quad (63)$$

$$Z_2 = \frac{e^{-i\sigma^0}}{\sqrt{\lambda^+\lambda^-}} \frac{i(\lambda^- - \lambda^+)}{e^{-2iZ^+} + e^{-2iZ^-}} \quad (64)$$

where we defined

$$\mathcal{Z}^\pm = \frac{1}{2} \left( \frac{\sigma^1 - \sigma^0}{\lambda^\pm - 1} + \frac{\sigma^1 + \sigma^0}{\lambda^\pm + 1} \right) \quad (65)$$

A two magnon (scattering) solution was also presented in [18] and discussed in section 4.

The form of this solution is

$$Z_1 = \frac{e^{i\sigma^0}}{2\sqrt{\lambda_1^+\lambda_2^+\lambda_1^-\lambda_2^-}} \frac{N_1}{D} \quad (66)$$

$$Z_2 = \frac{-i}{2\sqrt{\lambda_1^+\lambda_2^+\lambda_1^-\lambda_2^-}} \frac{N_2}{D} \quad (67)$$

with

$$D = \lambda_{12}^{++}\lambda_{12}^{--} \cosh(u_1 + u_2) + \lambda_{12}^{+-}\lambda_{12}^{-+} \cosh(u_1 - u_2) + \lambda_{11}^{+-}\lambda_{22}^{+-} \cos(v_1 - v_2) \quad (68)$$

$$N_1 = \lambda_{12}^{++}\lambda_{12}^{--} [\lambda_1^+\lambda_2^+ e^{+u_1+u_2} + \lambda_1^-\lambda_2^- e^{-u_1-u_2}] + \lambda_{12}^{-+}\lambda_{12}^{+-} [\lambda_1^+\lambda_2^- e^{+u_1-u_2} + \lambda_1^-\lambda_2^+ e^{-u_1+u_2}] + \lambda_1^+\lambda_1^-\lambda_{11}^{+-}\lambda_{22}^{+-} e^{i(v_1-v_2)} + \lambda_2^+\lambda_2^-\lambda_{11}^{+-}\lambda_{22}^{+-} e^{-i(v_1-v_2)} \quad (69)$$

$$N_2 = \lambda_{11}^{+-} e^{iv_1} [\lambda_{12}^{++}\lambda_{12}^{-+}\lambda_2^- e^{u_2} + \lambda_{12}^{--}\lambda_{12}^{+-}\lambda_2^+ e^{-u_2}] + \lambda_{22}^{+-} e^{iv_2} [\lambda_{21}^{++}\lambda_{21}^{-+}\lambda_1^- e^{u_1} + \lambda_{21}^{--}\lambda_{21}^{+-}\lambda_1^+ e^{-u_1}] \quad (70)$$

and

$$\lambda_{jk}^{\pm\pm} = \lambda_j^\pm - \lambda_k^\pm \quad (71)$$

$$u_j = i [\mathcal{Z}_j^+ - \mathcal{Z}_j^-] \quad (72)$$

$$v_j = \mathcal{Z}_j^+ + \mathcal{Z}_j^- - \sigma^0 \quad (73)$$

These solutions admit the following generalization:  $u_j \rightarrow u_j + a_j$  and  $v_j \rightarrow v_j + b_j$ , with  $a_j$  and  $b_j$  real. Two of these four parameter can be reabsorbed by a worldsheet coordinate redefinition. We are, therefore, left with two parameters corresponding to a relative distance and a relative phase.

The scattering solution presents the symmetry  $\lambda_1^+ \leftrightarrow \lambda_2^+$  or, alternatively  $\lambda_1^- \leftrightarrow \lambda_2^-$ . Also, it collapses to the single magnon solution for  $\lambda_j^+ = \lambda_j^-$  for  $j = 1$  or  $2$ .

## References

- [1] N. Beisert, R. Hernandez and E. Lopez, JHEP **0611**, 070 (2006) [arXiv:hep-th/0609044].
- [2] N. Beisert, B. Eden and M. Staudacher, J. Stat. Mech. **0701**, P021 (2007) [arXiv:hep-th/0610251].
- [3] B. Eden and M. Staudacher, J. Stat. Mech. **0611** (2006) P014 [arXiv:hep-th/0603157].
- [4] M. Staudacher, JHEP **0505**, 054 (2005) [arXiv:hep-th/0412188].
- [5] N. Beisert and M. Staudacher, Nucl. Phys. B **727**, 1 (2005) [arXiv:hep-th/0504190].
- [6] N. Beisert, arXiv:hep-th/0511082.
- [7] R. A. Janik, Phys. Rev. D **73**, 086006 (2006) [arXiv:hep-th/0603038].
- [8] G. Arutyunov and S. Frolov, Phys. Lett. B **639**, 378 (2006) [arXiv:hep-th/0604043].
- [9] G. Arutyunov, S. Frolov and M. Staudacher, JHEP **0410**, 016 (2004) [arXiv:hep-th/0406256].
- [10] N. Dorey, J. Phys. A **39**, 13119 (2006) [arXiv:hep-th/0604175].
- [11] H. Y. Chen, N. Dorey and K. Okamura, JHEP **0609**, 024 (2006) [arXiv:hep-th/0605155].
- [12] H. Y. Chen, N. Dorey and K. Okamura, JHEP **0611** (2006) 035 [arXiv:hep-th/0608047].
- [13] H. Y. Chen, N. Dorey and K. Okamura, arXiv:hep-th/0610295.
- [14] D. M. Hofman and J. M. Maldacena, J. Phys. A **39**, 13095 (2006) [arXiv:hep-th/0604135].
- [15] S. R. Coleman and H. J. Thun, Commun. Math. Phys. **61**, 31 (1978).
- [16] P. Dorey, arXiv:hep-th/9810026.
- [17] A. B. Zamolodchikov and A. B. Zamolodchikov, Annals Phys. **120** (1979) 253.



- [18] M. Spradlin and A. Volovich, JHEP **0610**, 012 (2006) [arXiv:hep-th/0607009].
- [19] L.D. Landau, Nuclear Phys. **13** (1959) 181.
- [20] R. E. Cutkosky, J. Math. Phys. **1** , (1960), 429.
- [21] D. Iagolnitzer, North Holland, 1978.
- [22] N. Beisert, V. Dippel and M. Staudacher, JHEP **0407** (2004) 075 [arXiv:hep-th/0405001].
- [23] A. Santambrogio and D. Zanon, Phys. Lett. B **545** (2002) 425 [arXiv:hep-th/0206079].  
D. Berenstein, D. H. Correa and S. E. Vazquez, JHEP **0602** (2006) 048 [arXiv:hep-th/0509015].
- [24] J. Maldacena and I. Swanson, arXiv:hep-th/0612079.
- [25] T. Klose and K. Zarembo, arXiv:hep-th/0701240.
- [26] C. Kalousios, M. Spradlin and A. Volovich, arXiv:hep-th/0611033.
- [27] G. Kalbermann, arXiv:cond-mat/0408198.
- [28] J. A. Minahan, arXiv:hep-th/0701005.
- [29] See for example: G. L. Lamb, “Elements of soliton theory”, Wiley Interscience, page 51
- [30] M. A. Olshanetsky and A. M. Perelomov, Phys. Rept. **71**, 313 (1981).
- [31] M. A. Olshanetsky and A. M. Perelomov, Phys. Rept. **94**, 313 (1983).
- [32] A. P. Polychronakos, J. Phys. A **39**, 12793 (2006) [arXiv:hep-th/0607033].
- [33] R. Hernandez and E. Lopez, JHEP **0607**, 004 (2006) [arXiv:hep-th/0603204].
- [34] I. Kostov, D. Serban and D. Volin, arXiv:hep-th/0703031.